

LONGITUDINAL BUNCH SHAPING AT PICOSECOND SCALES USING ALPHA-BBO CRYSTALS AT THE ADVANCED SUPERCONDUCTING TEST ACCELERATOR*

B.L. Beaudoin, Institute for Research in Electronics & Applied Physics, University of Maryland, College Park, MD 20742-3511, USA

D. Edstrom Jr., A.H. Lumpkin, J. Ruan, J. Thangaraj, Fermi National Accelerator Laboratory, Batavia, IL 60510-5011, USA

Abstract

The Integrable Optics Test Accelerator (IOTA) electron injector at Fermilab will enable a broad range of experiments at a national laboratory in order to study and develop solutions to the limitations that prevent the propagation of high intensity beams at picosecond lengths. One of the most significant complications towards increasing short-beam intensity is space-charge, especially in the vicinity of the gun. A few applications that require a longitudinally shaped electron beam at high intensities are for, the generation of THz waves and dielectric wakefields, each of which will encounter the effects of longitudinal space-charge. This paper investigates the effects of longitudinal space-charge on alpha-BBO UV laser shaped electron bunches in the vicinity of the 1½ cell 1.3 GHz cylindrically symmetric RF photocathode gun.

INTRODUCTION

The IOTA electron linac is currently being built and commissioned at Fermilab. As of March 27, 2015 they commissioned the electron linac up to 20 MeV, a laboratory record for maximum electron energy achieved [1]. The work presented in this paper seeks to answer the question: *How do density perturbations evolve and affect the electron beams 6-D beam phase-space brightness in a linear accelerator under various beam and machine conditions, such as acceleration?*

The University of Maryland Charged Particle Beam Laboratory has pioneered the ability of generating controlled perturbations to understand longitudinal space-charge an intense beams [2]. These controlled perturbations have ranged from grid modulations of a thermionic gun to UV laser focused onto the dispenser cathode, in-turn extracting additional current through photoemission and thus modulating a local region of the longer beam bunch [3-9]. This work intends to extend these studies to pico-second high current bunch lengths in the MeV range.

IOTA LASER & ELECTRON LINAC

IOTA facility houses a superconducting high intensity electron linear accelerator (linac). The first stage of the facility has generate and transported a 20 MeV intense

electron beam (shown in Fig. 1 below) using the accelerating cavity CAV2 [10]. Additional cavities are installed in the tunnel and conditioned that will allow the accelerator to transport up to 250 MeV electron beams.

Currently the electron linac is running with a Cs₂Te cathode for commissioning of the gun RF systems. A Cs₂Te photocathode is illuminated with an ultraviolet (263 μm) laser pulse, producing bunch trains at a repetition rate of 1-5 Hz and a frequency of 3 MHz for a 1 ms macro-pulse duration [11-12]. The number of bunches can be anywhere from 1-3000 depending on the beam charge.

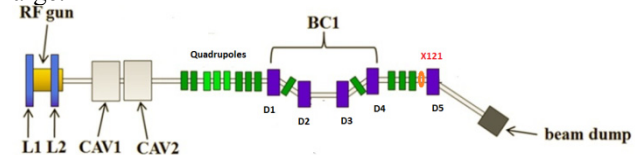


Figure 1: The 50 MeV electron beamline showing the RF gun followed by CAV1 and CAV2 that will accelerate the beam to 50 MeV. The green boxes show the quadrupoles used to focus the beam. The purple boxes are the dipoles that are used to bend the electron beam. D5 is the spectrometer dipole that is used in measuring the energy spectrum of the bunch. X121 is an Optical Transition Radiation (OTR) monitor that will be used to measure the current profile of the electron beam [11].

The photoinjector consists of a 1½ cell 1.3 GHz (L-band) cylindrical-symmetric RF gun injecting beam into the linac at nominally 5 MeV. By changing the gradient inside the RF gun, were able to generate beam energies ranging from 2-to-5 MeV.

TEMPORAL PULSE STACKING

The generation of longitudinally uniform electron beams can be achieved utilizing UV birefringent crystals by temporally stacking the incident laser pulse. The method of using birefringent crystals for temporal pulse stacking was developed at the Argonne Wakefield Accelerator (AWA) facility to generate 83-167 GHz electron bunch trains from an RF photocathode gun [13].

When a short laser pulse is incident on a birefringent crystal at a particular angle, the pulse will split into two pulses (or two rays), with different polarizations. The two pulses also separate in time as a result of the different group velocities. This separation in time can be calculated using Eqn. 1 below:

$$\Delta t = L \left(\frac{1}{v_{ge}} - \frac{1}{v_{go}} \right) \quad (1)$$

*Work supported by the University Research Association Inc.

Operated by the Fermi Research Alliance, LLC under Contract No. DE-AC02-07CH11359 with the United States Department of Energy

where, $v_{ge} = c/n_{ge}$ and $v_{go} = c/n_{go}$ are the group velocities, n_{ge} and n_{go} are the index of refractions for the different polarizations, c is the speed of light and L is the thickness of the crystal along the direction of propagation [13-14].

Temporal pulse stackers transform single Gaussian laser pulses into a train of pulses delayed in time. Depending on the number of crystals and parameters of each crystal, one can create a high frequency pulse train as in the case of the AWA facility or create a single pulse with a desired shape. Using three crystals with different lengths (18, 9, and 4.5 mm), we can take an incoming Gaussian laser pulse (as shown in Fig. 2a) and create a longitudinally uniform laser pulse (as shown in Fig. 2b) or a pulse train (as shown in Fig. 2c).

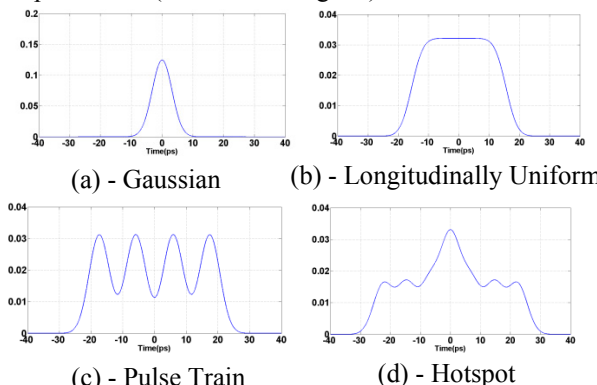


Figure 2a-d: (a) – Incoming gaussian laser pulse. (b) – Calculation of a longitudinally uniform laser pulse using three crystals with lengths (4.5, 9 and 18 mm). (c) – Calculation of a four pulse train using two crystals with lengths (13.3 and 27 mm). (d) – Calculation of a hotspot using three crystals with lengths (9, 18 and 25 mm).

BEAM-LINE MEASUREMENTS

The electron beam in these experiments is propagating from the source to the faraday cup diagnostic located 1.35 m from the gun at energies up to 5 MeV. The facility has four birefringent crystals of length, 4.5, 9, 18 and 25 mm. We have experimentally generated electron bunches with laser profiles such as, flattop, doublet, triplet, hotspot, etc.

Figure 3, illustrates the initial measurements of a doublet distribution formed using three birefringent crystals. The three crystals (4.5, 9 and 18 mm) were oriented at -52.7° , -15.9° and -86.1° respectively [15]. The separation of the peaks in the doublet, measured on the streak camera in the laser lab was 21 ps. The sigma's of the individual peaks was 5.4 ps (or 9.4 ps rms) and 4.4 ps (or 7.6 ps rms) [15]. The charge was collected using the faraday cup diagnostic for different gun gradients ranging from 25 MV/m to 45 MV/m (corresponding to beam energies of 2.5 MeV to 4.8 MeV).

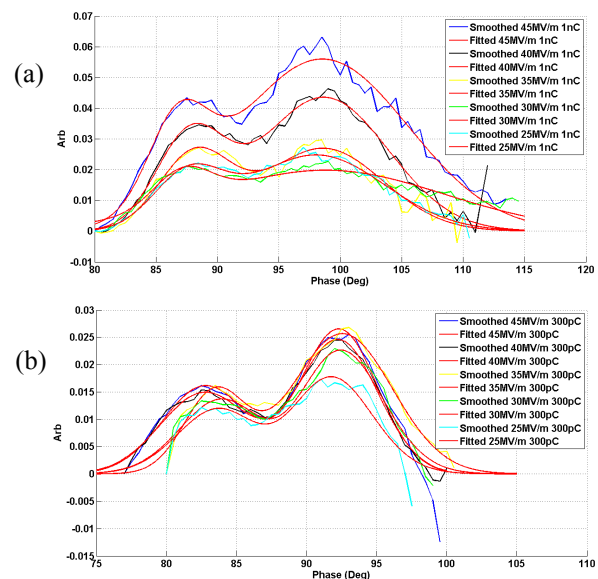


Figure 3a-b: Gun phase measurements for 1 nC bunch (a) and 300 pC bunch (b) collected using the faraday cup diagnostic for different gun gradients ranging from 25 MV/m to 45 MV/m (corresponding to beam energies of 2.5 MeV to 4.8 MeV). One degree corresponds to 2.14 ps for the L-band photoinjector.

In this measurement, the gun drive phase is scanned over a range of phases such that the peak electric field moves relative to the drive laser pulse. The charge is then collected with a faraday cup. This measurement is not ideal as it infers the longitudinal distribution through the gun phase but it provides some insight into the effect of longitudinal space-charge. The raw data from the faraday cup is then differentiated to observe the longitudinal distribution imposed by the birefringent crystals in the laser lab. The data is then differentiated since the faraday cup has a long time constant.

The difference of the peaks (shown in Fig. 3a) for the gun phase measurements of the 1 nC bunch is illustrated below in Figure 4 for three of the five gun gradients. The lowest two gradients (25 and 30 MV/m) were not distinguishable.

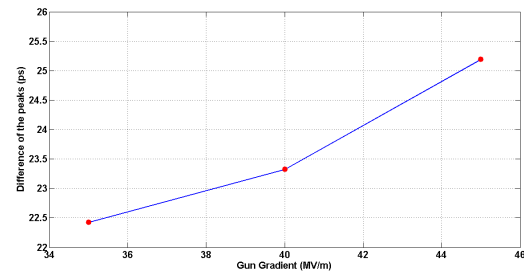


Figure 4: Separation between peaks for the 1 nC bunch gun phase measurements (shown in Fig. 3a). Only three points are shown as the peaks for gun gradients of 25 and 30 MV/m were not distinguishable.

The gun gradient was decreased over a range, allowing longitudinal space-charge forces to increase over that same range. This resulted in a decrease in the separation between the peaks. Longitudinal space-charge washed out the doublet distribution at 1 nC and low beam energies. The same experiment was repeated at a low charge (300 pC) with little separation between peaks.

As a sanity check, the gun phase measurement and differentiation method was repeated without the crystals to verify that the technique could in fact discern the gaussian distribution of the incoming laser pulse. This check was successful.

CONCLUSION

The initial measurements presented in this study have illustrated that longitudinal space-charge forces are present. There are some concerns with the inferred gun phase scan measurement as it is unclear as to what the limiting resolution of the diagnostic is. Other similar experiments with doublet distributions separated by 3-4 ps were unresolvable using the gun phase scan technique but were resolvable in the laser lab streak camera [16]. ASTRA simulation runs are ongoing in order to successfully reproduce the gun phase scans and gain insight through longitudinal phase-space images of the various beam distributions created and their evolution through the machine.

The 20 MeV beam-line is operational and the next stage of experiments requires propagating beam down the line and characterizing the various longitudinal distributions as a function of beam energy and charge at the streak camera located at X121 and the spectrometer magnet at the end of the line.

ACKNOWLEDGMENT

I would like to thank the IOTA team at Fermilab for the use of the superconducting electron linac, without which this work would not have been possible.

REFERENCES

- [1] <https://www-bd.fnal.gov/Elog/?entryIDs=47803&logNames=IOTA+ASTA>
- [2] M. Reiser, *Theory and Design of Charged Particle Beams* 2nd Ed. (Wiley-VCH Inc., Weinheim Germany, 2008) p.413.
- [3] Y. Huo, Masters Thesis, University of Maryland, (2004).
- [4] J.R. Harris, J.G. Neumann and P.G. O'Shea, *Journal of Applied Physics*, **99**, 093306, (2006).
- [5] J. C. T. Thangaraj, G. Bai, B.L. Beaudoin, S. Bernal, D.W. Feldman, R. Fiorito, I. Haber, R.A.

Kishek, P.G. O'Shea, M. Reiser, D. Stratakis, K. Tian, and M. Walter, *Proceedings of the 2007 Particle Accelerator Conference*, Albuquerque, 2007 (IEEE, New York, 2007).

- [6] J. C. T. Thangaraj, Ph.D. Dissertation, University of Maryland, 2009.
- [7] B.L. Beaudoin, S. Bernal, I. Haber, R.A. Kishek, P.G. O'Shea, M. Reiser, J.C.T. Thangaraj, K. Tian, M. Walter and C. Wu, *Proceedings of the 2007 Particle Accelerator Conference*, Albuquerque, 2007 (IEEE, New York, 2007).
- [8] B. Beaudoin, Masters Thesis, University of Maryland, 2008.
- [9] B. Beaudoin, Ph.D. Dissertation, University of Maryland, 2011.
- [10] J. Branlard, B. Chase, G. Cancelo, R. Carcagno, H. Edwards, R. Fliller, B. Hanna, E. Harms, A. Hocker, T. Koeth, M. Kucera, A. Makulski, U. Mavric, M. McGee, A. Paytyan, Y. Pischalnikov, P. Prieto, R. Rechenmacher, J. Reid, N. Wilcer, K. Treptow, T. Zmuda, "Capture Cavity II Results at FNAL", *Proceedings of the 2007 Particle Accelerator Conference*, Albuquerque, 2007 (IEEE, New York, 2007).
- [11] Proposal from Fermilab for an: *Accelerator R&D User Facility at Fermilab's Advanced Superconducting Test Accelerator (ASTA)*, (2013).
- [12] J. Li, R. Tikhoplav, A. Melissinos, "Performance of the upgraded laser system for the Fermilab-NIU photoinjector", *Nucl. Instr. and Meth. A* **564** (2006) p. 57.
- [13] J.G. Power, C. Jing, I. Jovanovic, "High Frequency Bunch Train Generation from an RF Photoinjector at the AWA", *Proceedings of the 2009 Particle Accelerator Conference*, Vancouver, 2009 (IEEE, New York, 2009).
- [14] J. Thangaraj, D. Edstrom, A.H. Lumpkin, J. Ruan, B. Beaudoin, "Z-Shaper: A Picosecond UV Laser Pulse Shaping Channel at the Advanced Superconducting Test Accelerator", *Proceedings of LINAC2014*, Geneva, Switzerland, 2014.
- [15] NML Electronic Logbook, <http://dbweb4.fnal.gov:8080/ECL/nml/E/show?e=7857>
- [16] NML Electronic Logbook, <http://dbweb4.fnal.gov:8080/ECL/nml/E/show?e=8239>